Supplementary Information (SI) for Journal of Materials Chemistry C.
This journal is © The Royal Society of Chemistry 2026

# Supplementary Information

## A Theoretical Framework for Benchmarking Amphiphilic 2D Covalent Organic Frameworks for Atmospheric Water Harvesting

Nouf Eid Alshaikh[a], Ismail Abdulazeez[b]*, Niaz Ali Khan[b], Billel Salhi[b], Nadeem Baig[b], Abdulrahman Albetar[a]*

[a]*Chemistry Department, King Fahd University of Petroleum and Minerals, Dhahran 31261, Saudi Arabia.*

[b]*Interdisciplinary Research Centre for Membranes and Water Security, King Fahd University of Petroleum and Minerals, Dhahran, 31261, Saudi Arabia.*

*Corresponding Authors: Dr. Ismail Abdulazeez (ismail.abdulazeez@kfupm.edu.sa); Dr. Abdulrahman Albetar (abetar@kfupm.edu.sa).

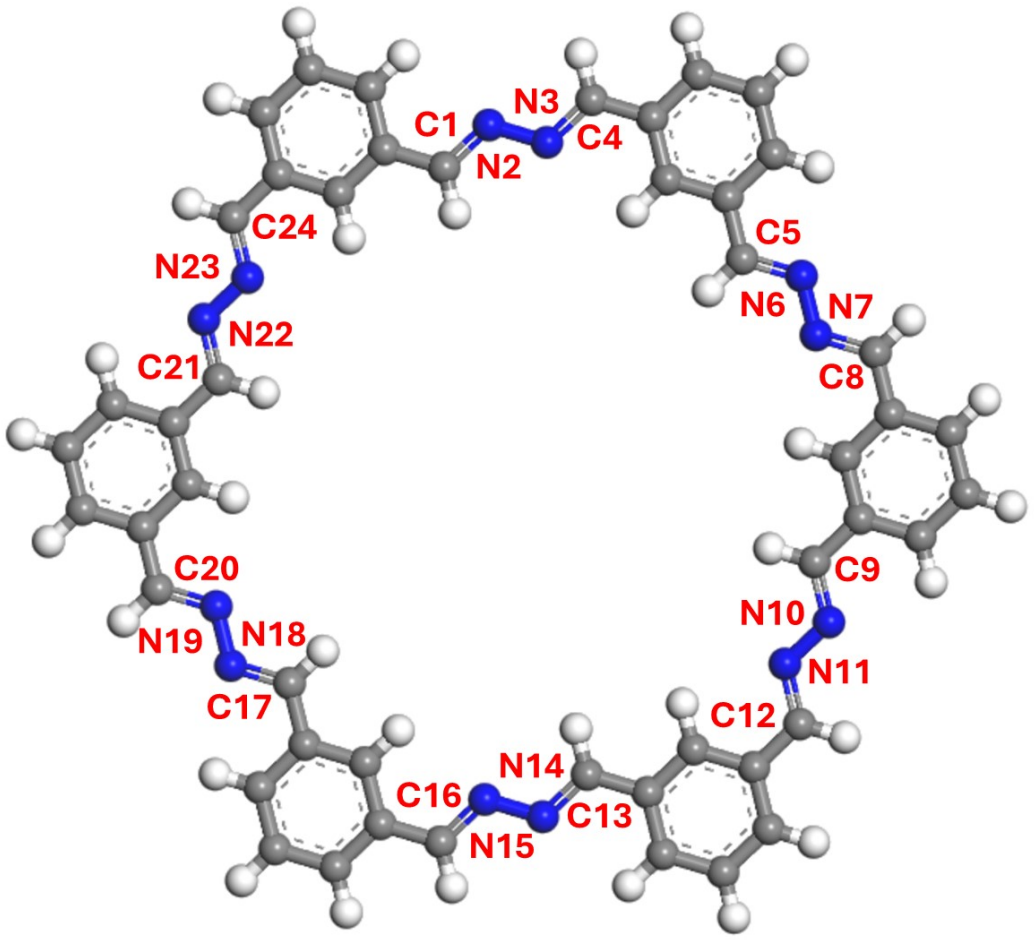


**Figure S1**: Atom labeling scheme of AB-COF, used for analyzing changes in bond properties

**Table S1**: Structural properties of the investigated COFs calculated at the B3LYP/6-311g(d) level of theory

| Atoms | AB-COF | MN-COF | $MN_2$-COF | $M_2N$-COF | FN-COF | $FN_2$-COF | $F_2N$-COF | M-COF | N-COF |
|---|---|---|---|---|---|---|---|---|---|
| Bond lengths (Å) | | | | | | | | | |
| $C_1$-$N_2$ | 1.283 | 1.289 | 1.286 | 1.286 | 1.289 | 1.290 | 1.284 | 1.286 | 1.287 |
| $N_2$-$N_3$ | 1.390 | 1.391 | 1.388 | 1.394 | 1.388 | 1.386 | 1.392 | 1.393 | 1.387 |
| $N_3$-$C_4$ | 1.283 | 1.283 | 1.290 | 1.282 | 1.278 | 1.278 | 1.278 | 1.282 | 1.290 |
| $C_5$-$N_6$ | 1.283 | 1.286 | 1.288 | 1.286 | 1.283 | 1.283 | 1.283 | 1.286 | 1.287 |
| $N_6$-$N_7$ | 1.390 | 1.388 | 1.387 | 1.388 | 1.387 | 1.387 | 1.386 | 1.394 | 1.387 |
| $N_7$-$C_8$ | 1.283 | 1.291 | 1.291 | 1.291 | 1.292 | 1.292 | 1.292 | 1.282 | 1.290 |
| $C_9$-$N_{10}$ | 1.283 | 1.289 | 1.289 | 1.289 | 1.289 | 1.287 | 1.289 | 1.286 | 1.288 |
| $N_{10}$-$N_{11}$ | 1.390 | 1.392 | 1.392 | 1.392 | 1.387 | 1.386 | 1.387 | 1.394 | 1.387 |
| $N_{11}$-$C_{12}$ | 1.283 | 1.282 | 1.283 | 1.282 | 1.278 | 1.292 | 1.278 | 1.282 | 1.290 |
| $C_{13}$-$N_{14}$ | 1.283 | 1.286 | 1.286 | 1.286 | 1.283 | 1.290 | 1.283 | 1.286 | 1.288 |
| $N_{14}$-$N_{15}$ | 1.390 | 1.388 | 1.388 | 1.394 | 1.386 | 1.386 | 1.392 | 1.394 | 1.387 |
| $N_{15}$-$C_{16}$ | 1.283 | 1.291 | 1.291 | 1.282 | 1.292 | 1.278 | 1.277 | 1.282 | 1.290 |
| $C_{17}$-$N_{18}$ | 1.283 | 1.288 | 1.288 | 1.286 | 1.289 | 1.283 | 1.283 | 1.286 | 1.288 |
| $N_{18}$-$N_{19}$ | 1.390 | 1.392 | 1.387 | 1.388 | 1.387 | 1.387 | 1.386 | 1.394 | 1.387 |
| $N_{19}$-$C_{20}$ | 1.283 | 1.283 | 1.291 | 1.291 | 1.278 | 1.291 | 1.292 | 1.282 | 1.290 |
| $C_{21}$-$N_{22}$ | 1.283 | 1.286 | 1.286 | 1.289 | 1.283 | 1.287 | 1.289 | 1.286 | 1.288 |
| $N_{22}$-$N_{23}$ | 1.390 | 1.387 | 1.392 | 1.391 | 1.387 | 1.386 | 1.387 | 1.394 | 1.387 |
| $N_{23}$-$C_{24}$ | 1.283 | 1.291 | 1.283 | 1.282 | 1.292 | 1.292 | 1.278 | 1.282 | 1.290 |
| Bond angles (°) | | | | | | | | | |
| $C_1$-$N_2$-$N_3$ | 112.5 | 110.3 | 111.3 | 110.4 | 110.2 | 110.0 | 110.6 | 110.3 | 111.3 |
| $N_2$-$N_3$-$C_4$ | 112.6 | 114.3 | 114.6 | 114.1 | 114.7 | 115.1 | 113.9 | 114.1 | 114.5 |
| $C_5$-$N_6$-$N_7$ | 112.5 | 111.2 | 111.3 | 111.3 | 111.9 | 111.8 | 112.2 | 110.3 | 111.4 |
| $N_6$-$N_7$-$C_8$ | 112.6 | 114.6 | 114.6 | 114.6 | 113.7 | 113.9 | 113.5 | 114.2 | 114.6 |
| $C_9$-$N_{10}$-$N_{11}$ | 112.5 | 110.2 | 110.3 | 110.2 | 110.2 | 111.8 | 110.3 | 110.3 | 111.3 |
| $N_{10}$-$N_{11}$-$C_{12}$ | 112.6 | 114.5 | 114.2 | 114.5 | 114.8 | 114.0 | 114.6 | 114.2 | 114.5 |
| $C_{13}$-$N_{14}$-$N_{15}$ | 112.5 | 111.3 | 111.4 | 110.2 | 111.9 | 110.0 | 110.6 | 110.2 | 111.4 |
| $N_{14}$-$N_{15}$-$C_{16}$ | 112.6 | 114.5 | 114.5 | 114.2 | 113.8 | 115.1 | 113.9 | 114.3 | 114.6 |
| $C_{17}$-$N_{18}$-$N_{19}$ | 112.5 | 110.3 | 111.2 | 111.2 | 110.2 | 111.7 | 112.2 | 110.1 | 111.3 |
| $N_{18}$-$N_{19}$-$C_{20}$ | 112.6 | 114.3 | 114.7 | 114.7 | 114.8 | 113.9 | 113.5 | 114.3 | 114.6 |
| $C_{21}$-$N_{22}$-$N_{23}$ | 112.5 | 111.4 | 110.3 | 110.3 | 111.9 | 111.8 | 110.3 | 110.2 | 111.3 |
| $N_{22}$-$N_{23}$-$C_{24}$ | 112.6 | 114.5 | 114.3 | 114.3 | 113.7 | 114.0 | 114.6 | 114.2 | 114.6 |

**Table S2**: Structural properties of the investigated COFs calculated at the M06/6-311g(d) level of theory

| Selected atoms | AB-COF | MN-COF | $MN_2$-COF | $M_2N$-COF | FN-COF | $FN_2$-COF | $F_2N$-COF | M-COF | N-COF |
|---|---|---|---|---|---|---|---|---|---|
| Bond lengths | | | | | | | | | |
| $C_1$-$N_2$ | 1.278 | 1.284 | 1.281 | 1.281 | 1.278 | 1.278 | 1.283 | 1.281 | 1.282 |
| $N_2$-$N_3$ | 1.384 | 1.385 | 1.382 | 1.382 | 1.381 | 1.381 | 1.381 | 1.387 | 1.381 |
| $N_3$-$C_4$ | 1.278 | 1.278 | 1.285 | 1.286 | 1.287 | 1.286 | 1.274 | 1.278 | 1.285 |
| $C_5$-$N_6$ | 1.278 | 1.281 | 1.282 | 1.283 | 1.284 | 1.282 | 1.276 | 1.281 | 1.282 |
| $N_6$-$N_7$ | 1.383 | 1.382 | 1.382 | 1.385 | 1.380 | 1.381 | 1.354 | 1.387 | 1.382 |
| $N_7$-$C_8$ | 1.278 | 1.286 | 1.285 | 1.278 | 1.273 | 1.286 | 1.273 | 1.277 | 1.285 |
| $C_9$-$N_{10}$ | 1.278 | 1.284 | 1.284 | 1.281 | 1.278 | 1.285 | 1.279 | 1.281 | 1.282 |
| $N_{10}$-$N_{11}$ | 1.384 | 1.385 | 1.385 | 1.387 | 1.381 | 1.379 | 1.379 | 1.387 | 1.381 |
| $N_{11}$-$C_{12}$ | 1.278 | 1.278 | 1.278 | 1.277 | 1.287 | 1.273 | 1.287 | 1.277 | 1.285 |
| $C_{13}$-$N_{14}$ | 1.278 | 1.281 | 1.280 | 1.281 | 1.285 | 1.278 | 1.284 | 1.281 | 1.282 |
| $N_{14}$-$N_{15}$ | 1.384 | 1.382 | 1.382 | 1.382 | 1.379 | 1.381 | 1.380 | 1.387 | 1.382 |
| $N_{15}$-$C_{16}$ | 1.278 | 1.286 | 1.285 | 1.286 | 1.272 | 1.286 | 1.271 | 1.278 | 1.285 |
| $C_{17}$-$N_{18}$ | 1.278 | 1.283 | 1.282 | 1.283 | 1.278 | 1.282 | 1.277 | 1.281 | 1.282 |
| $N_{18}$-$N_{19}$ | 1.384 | 1.385 | 1.381 | 1.385 | 1.381 | 1.381 | 1.382 | 1.387 | 1.381 |
| $N_{19}$-$C_{20}$ | 1.278 | 1.278 | 1.285 | 1.278 | 1.286 | 1.286 | 1.270 | 1.277 | 1.285 |
| $C_{21}$-$N_{22}$ | 1.278 | 1.281 | 1.284 | 1.281 | 1.284 | 1.285 | 1.277 | 1.281 | 1.283 |
| $N_{22}$-$N_{23}$ | 1.384 | 1.382 | 1.385 | 1.387 | 1.381 | 1.379 | 1.381 | 1.387 | 1.381 |
| $N_{23}$-$C_{24}$ | 1.278 | 1.286 | 1.278 | 1.277 | 1.272 | 1.272 | 1.288 | 1.277 | 1.285 |
| Bond angles (°) | | | | | | | | | |
| $C_1$-$N_2$-$N_3$ | 112.3 | 110.0 | 111.2 | 111.0 | 112.1 | 111.5 | 110.9 | 110.0 | 111.0 |
| $N_2$-$N_3$-$C_4$ | 112.3 | 114.1 | 114.1 | 114.3 | 113.0 | 113.6 | 113.6 | 113.9 | 114.4 |
| $C_5$-$N_6$-$N_7$ | 112.3 | 111.2 | 111.1 | 110.0 | 109.9 | 111.5 | 116.6 | 110.0 | 111.0 |
| $N_6$-$N_7$-$C_8$ | 112.3 | 114.1 | 114.3 | 114.2 | 114.9 | 113.8 | 116.8 | 114.1 | 114.2 |
| $C_9$-$N_{10}$-$N_{11}$ | 112.3 | 110.0 | 109.9 | 110.0 | 111.8 | 109.8 | 111.5 | 110.1 | 111.2 |
| $N_{10}$-$N_{11}$-$C_{12}$ | 112.3 | 114.2 | 114.2 | 114.1 | 113.4 | 115.3 | 113.7 | 114.0 | 114.2 |
| $C_{13}$-$N_{14}$-$N_{15}$ | 112.3 | 111.1 | 110.9 | 111.0 | 109.9 | 111.5 | 109.4 | 110.1 | 111.1 |
| $N_{14}$-$N_{15}$-$C_{16}$ | 112.3 | 114.2 | 114.4 | 114.3 | 115.1 | 113.6 | 115.4 | 113.9 | 114.1 |
| $C_{17}$-$N_{18}$-$N_{19}$ | 112.3 | 110.0 | 110.9 | 110.0 | 111.7 | 111.5 | 110.5 | 109.9 | 111.1 |
| $N_{18}$-$N_{19}$-$C_{20}$ | 112.3 | 114.2 | 114.5 | 114.2 | 113.3 | 113.8 | 114.4 | 114.1 | 114.4 |
| $C_{21}$-$N_{22}$-$N_{23}$ | 112.3 | 111.2 | 110.0 | 110.1 | 109.8 | 109.7 | 112.8 | 110.0 | 111.1 |
| $N_{22}$-$N_{23}$-$C_{24}$ | 112.3 | 114.1 | 114.2 | 114.1 | 114.9 | 115.3 | 112.3 | 114.0 | 114.5 |

**Table S3**: Frontier orbitals of the investigated COFs calculated at the B3LYP and M06/6-311g(d) levels of theory

| COFs | HOMO | LUMO |
|---|---|---|
| **AB-COF** | 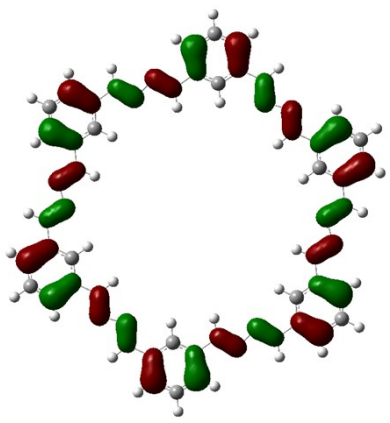 | 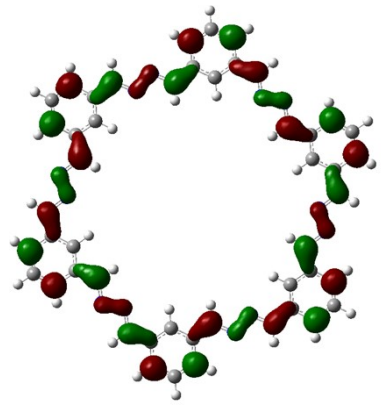 |
| **MN-COF** | 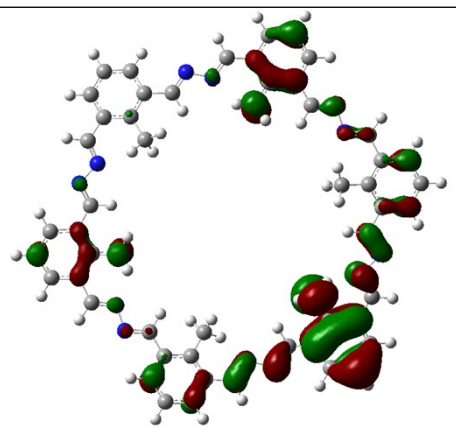 | 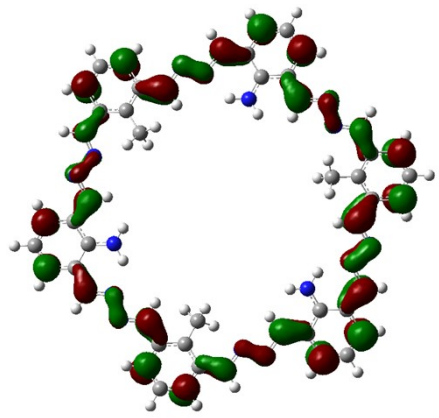 |
| **$MN_2$-COF** | 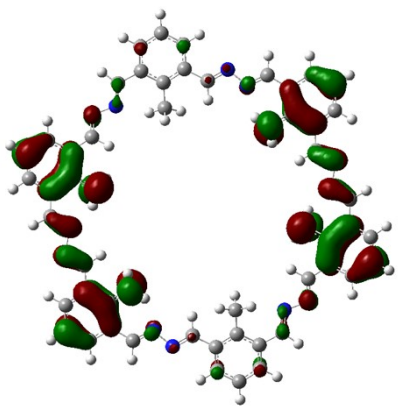 | 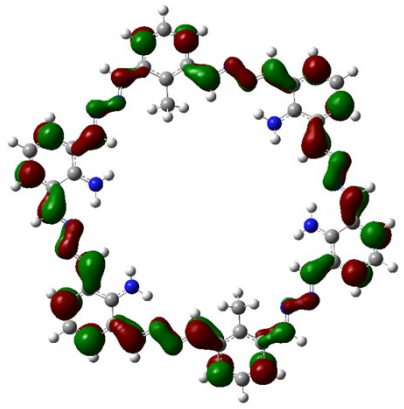 |
| **$M_2N$-COF** | 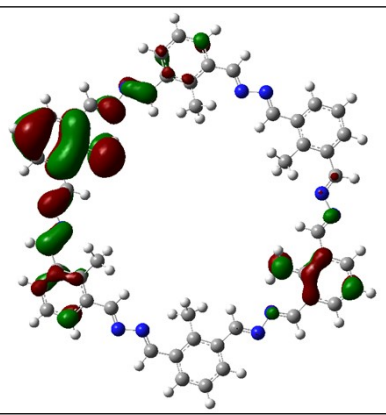 | 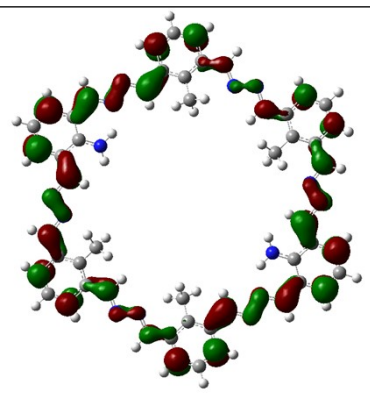 |

| | | |
|---|---|---|
| **FN-COF** | 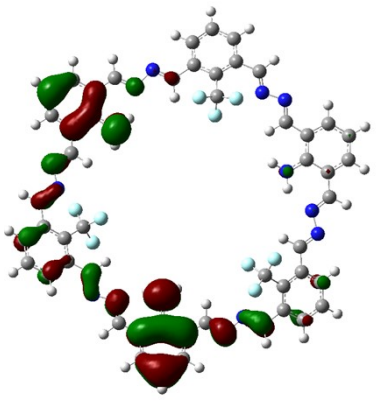 | 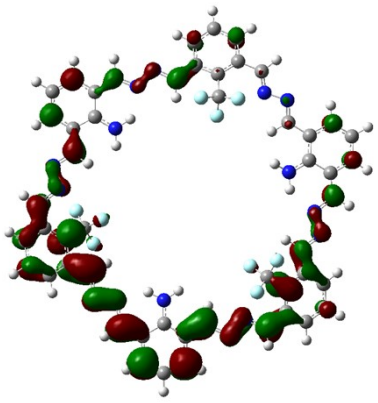 |
| **$FN_2$-COF** | 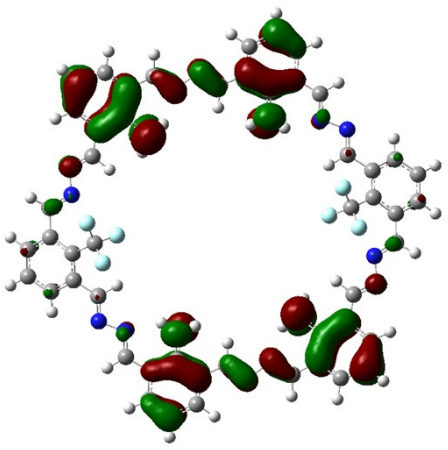 | 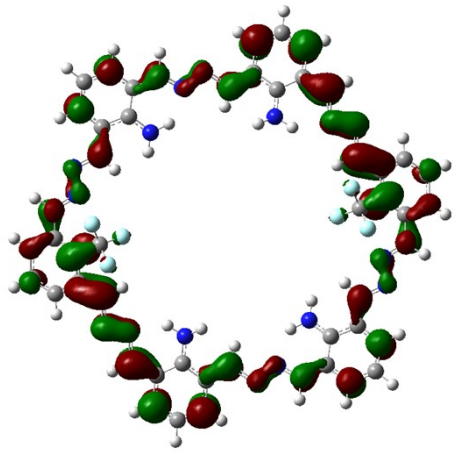 |
| **$F_2N$-COF** | 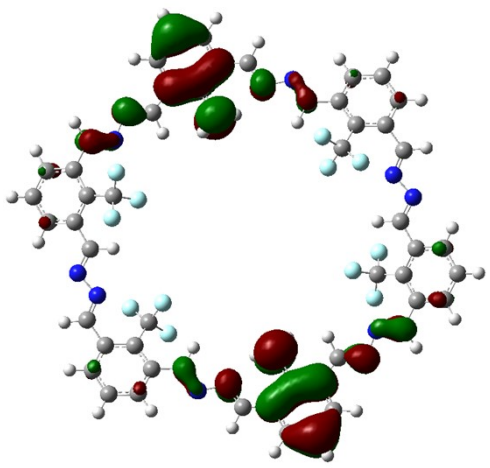 | 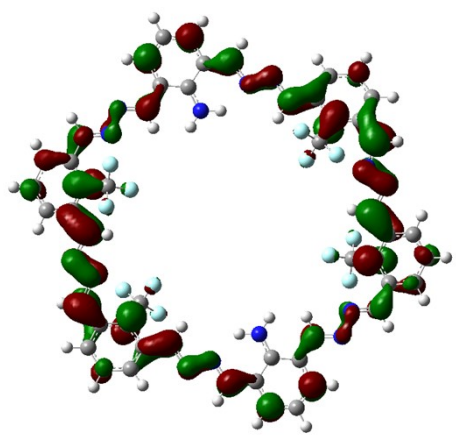 |
| **M-COF** | 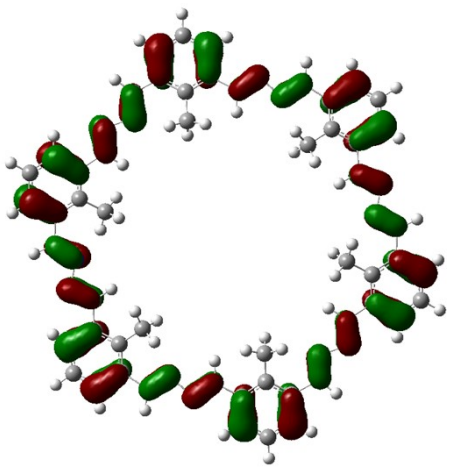 | 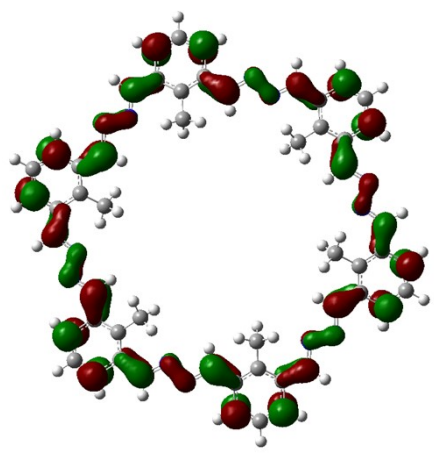 |
| **N-COF** | 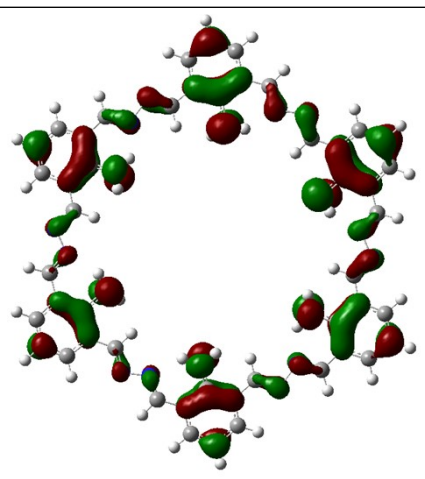 | 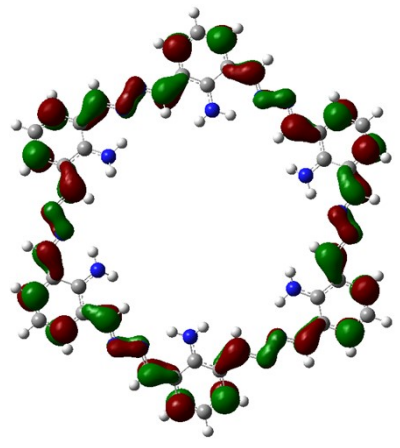 |

**Table S4**: Electronic properties of the investigated COFs calculated at the B3LYP/6-311g(d) level of theory

| COFs | $E_{HOMO}$ (eV) | $E_{LUMO}$ (eV) | ΔE (eV) | I (eV) | A (eV) | χ (eV) | η (eV) | Dipole moment (Debye) |
|---|---|---|---|---|---|---|---|---|
| AB-COF | -6.360 | -2.561 | 3.799 | 6.360 | 2.561 | 4.461 | 1.900 | 0.0002 |
| MN-COF | -5.774 | -2.460 | 3.314 | 5.774 | 2.460 | 4.117 | 1.657 | 0.9384 |
| $MN_2$-COF | -5.687 | -2.468 | 3.220 | 5.687 | 2.468 | 4.077 | 1.610 | 0.0709 |
| $M_2N$-COF | -5.790 | -2.451 | 3.340 | 5.790 | 2.451 | 4.120 | 1.670 | 0.1808 |
| FN-COF | -5.831 | -2.592 | 3.240 | 5.831 | 2.592 | 4.212 | 1.620 | 1.0257 |
| $FN_2$-COF | -5.690 | -2.573 | 3.117 | 5.690 | 2.573 | 4.131 | 1.559 | 2.4068 |
| $F_2N$-COF | -5.865 | -2.648 | 3.217 | 5.865 | 2.648 | 4.256 | 1.609 | 0.0059 |
| M-COF | -6.287 | -2.428 | 3.859 | 6.287 | 2.428 | 4.358 | 1.929 | 0.4361 |
| N-COF | -5.613 | -2.482 | 3.131 | 5.613 | 2.482 | 4.048 | 1.565 | 0.0476 |

**Table S5**: Electronic properties of the investigated COFs calculated at the M06/6-311g(d) level of theory

| COFs | $E_{HOMO}$ (eV) | $E_{LUMO}$ (eV) | ΔE (eV) | I (eV) | A (eV) | χ (eV) | η (eV) | Dipole moment (Debye) |
|---|---|---|---|---|---|---|---|---|
| AB-COF | -6.6720 | -2.4107 | 4.2613 | 6.6720 | 2.4107 | 4.5413 | 2.1307 | 0.0001 |
| MN-COF | -6.1000 | -2.3171 | 3.7829 | 6.1000 | 2.3171 | 4.2085 | 1.8915 | 0.1932 |
| $MN_2$-COF | -5.9903 | -2.3233 | 3.6670 | 5.9903 | 2.3233 | 4.1568 | 1.8335 | 0.7298 |
| $M_2N$-COF | -6.1136 | -2.3089 | 3.8047 | 6.1136 | 2.3089 | 4.2112 | 1.9023 | 0.0011 |
| FN-COF | -6.1680 | -2.4278 | 3.7402 | 6.1680 | 2.4278 | 4.2979 | 1.8701 | 2.2104 |
| $FN_2$-COF | -6.0175 | -2.4134 | 3.6041 | 6.0175 | 2.4134 | 4.2155 | 1.8021 | 1.8906 |
| $F_2N$-COF | -6.1925 | -2.4403 | 3.7522 | 6.1925 | 2.4403 | 4.3164 | 1.8761 | 2.5750 |
| M-COF | -6.5952 | -2.2841 | 4.3111 | 6.5952 | 2.2841 | 4.4397 | 2.1556 | 0.2482 |
| N-COF | -5.9261 | -2.3356 | 3.5905 | 5.9261 | 2.3356 | 4.1308 | 1.7953 | 0.7219 |

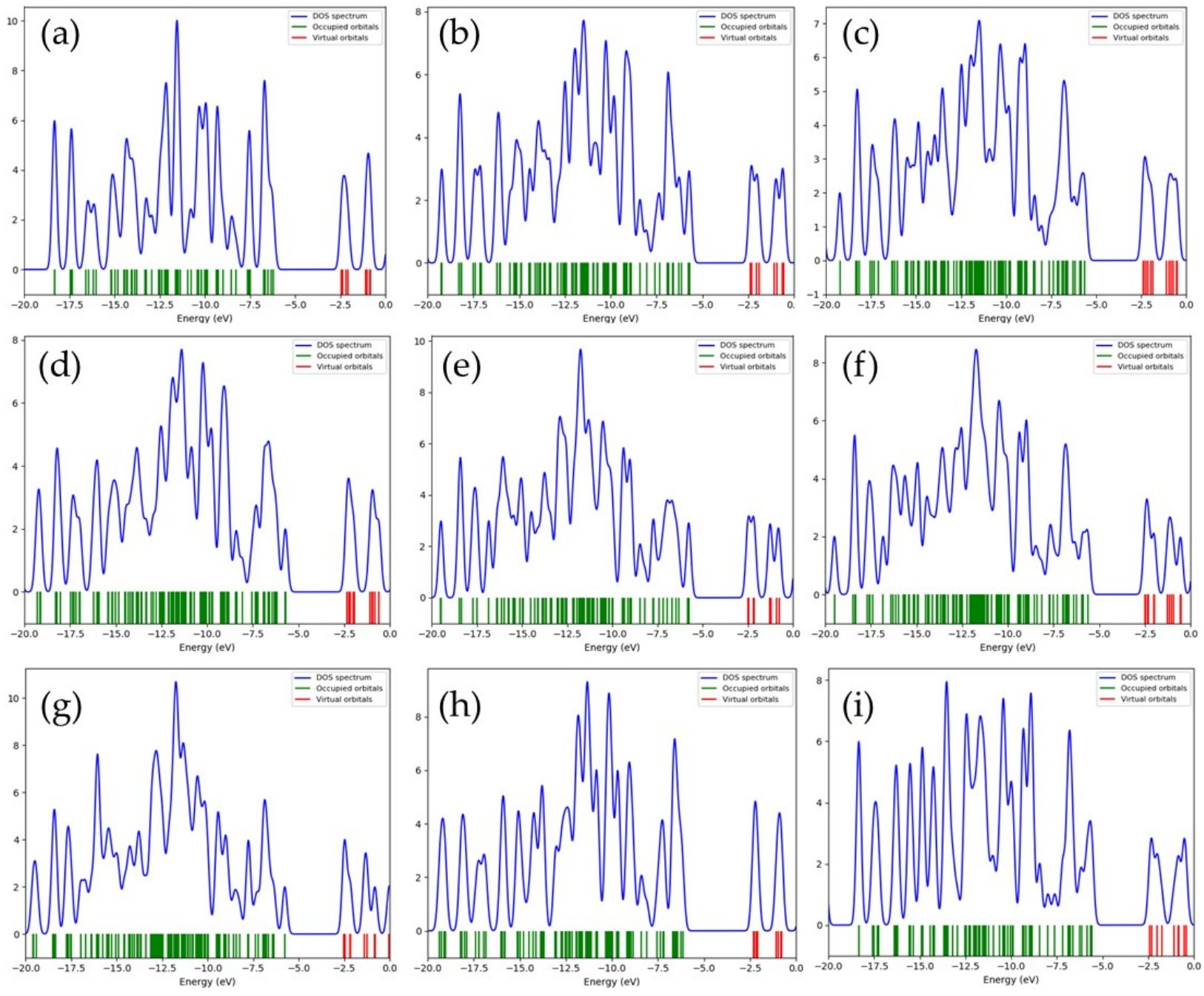


**Figure S2**: Density of States (DOS) spectra of the investigated (a) AB-COF, (b) MN-COF, (c) $MN_2$-COF, (d) $M_2N$-COF, (e) FN-COF, (f) $FN_2$-COF, (g) $F_2N$-COF, (h) M-COF and (i) N-COF calculated at the B3LYP/6-311g(d) level of theory

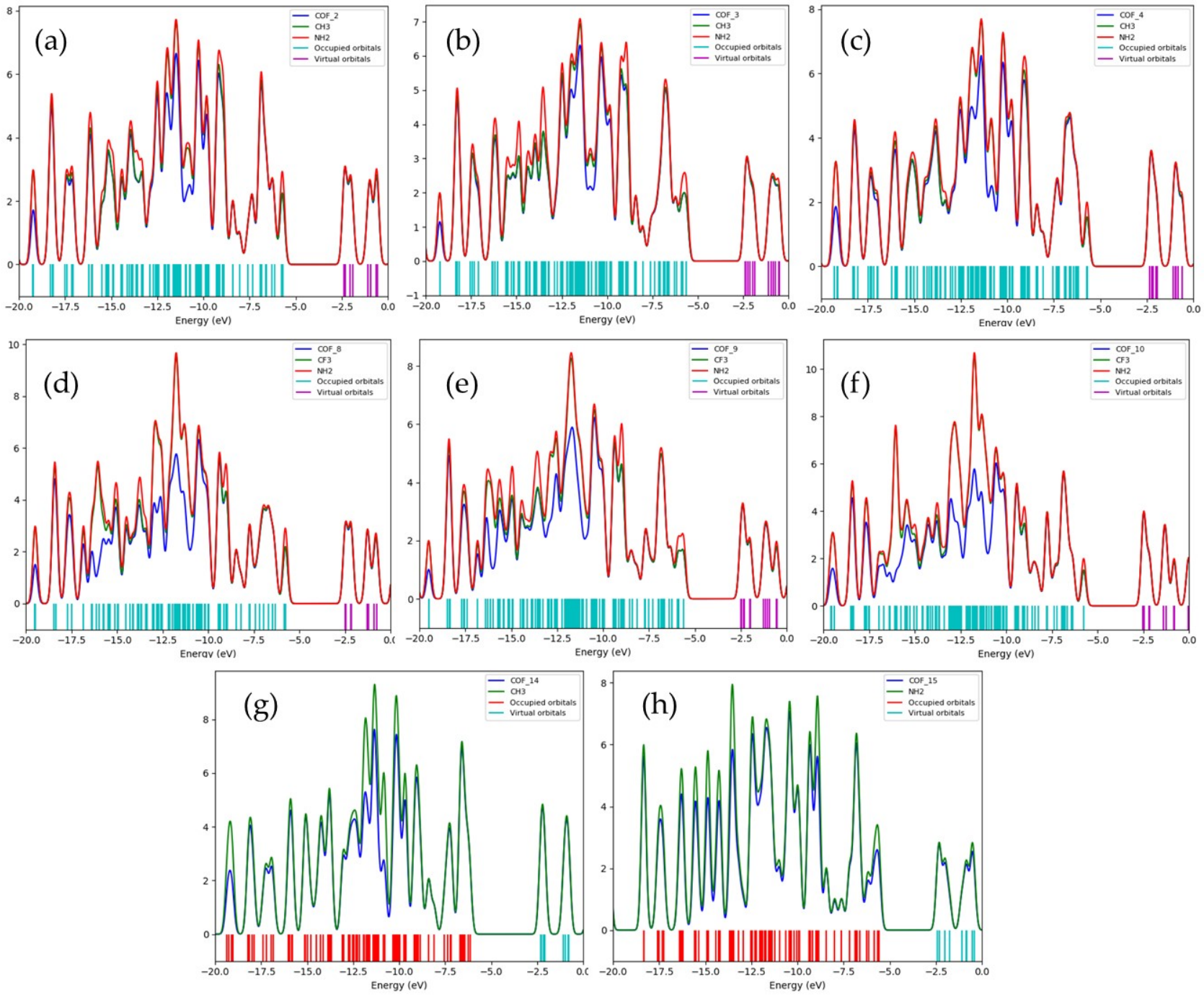


**Figure S3**: Projected Density of States (PDOS) spectra of the investigated (a) MN-COF, (b) $MN_2$-COF, (c) $M_2N$-COF, (d) FN-COF, (e) $FN_2$-COF, (f) $F_2N$-COF, (g) M-COF and (h) N-COF calculated at the B3LYP/6-311g(d) level of theory

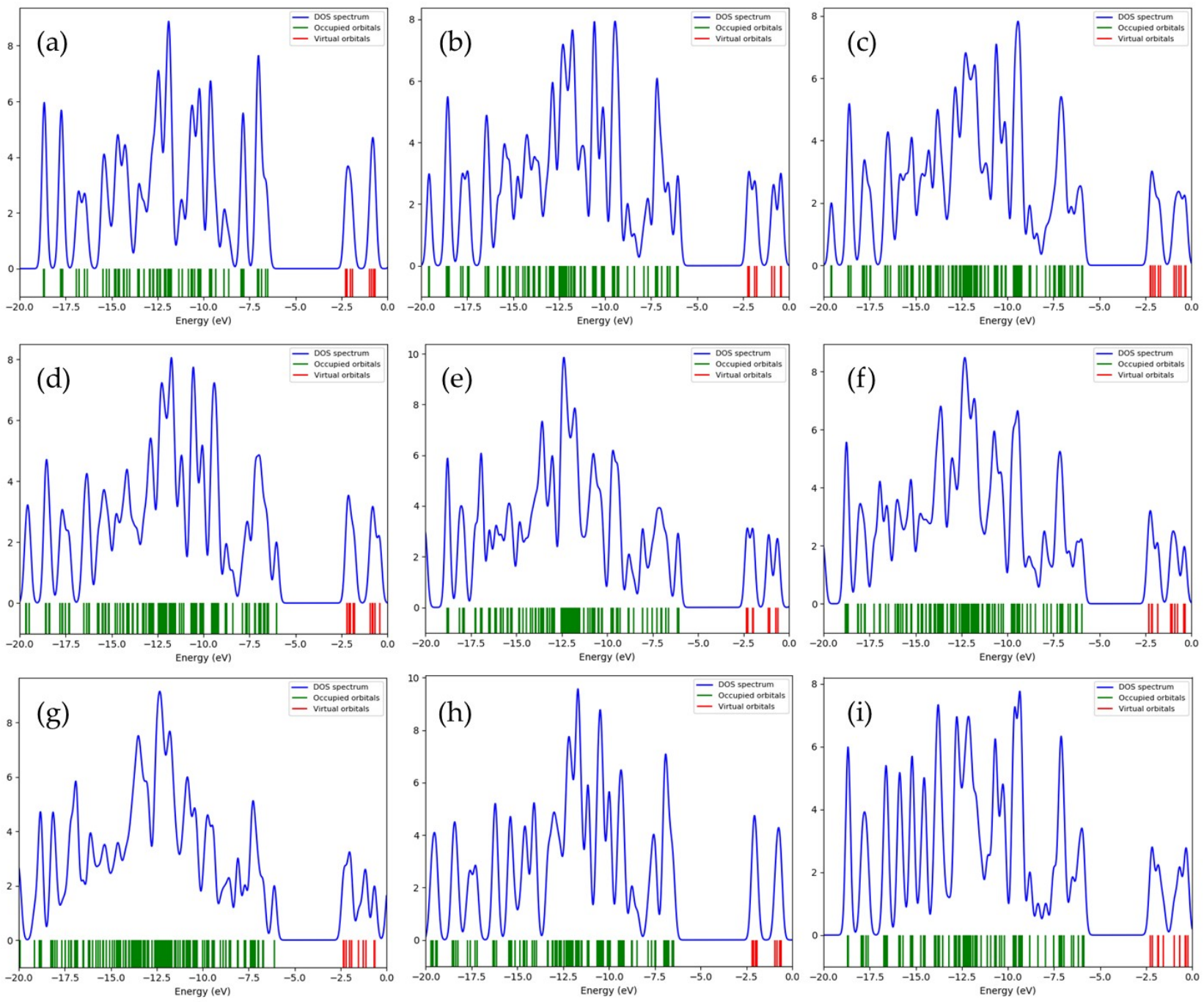


**Figure S4**: Density of States (DOS) spectra of the investigated (a) AB-COF, (b) MN-COF, (c) $MN_2$-COF, (d) $M_2N$-COF, (e) FN-COF, (f) $FN_2$-COF, (g) $F_2N$-COF, (h) M-COF and (i) N-COF calculated at the M06/6-311g(d) level of theory

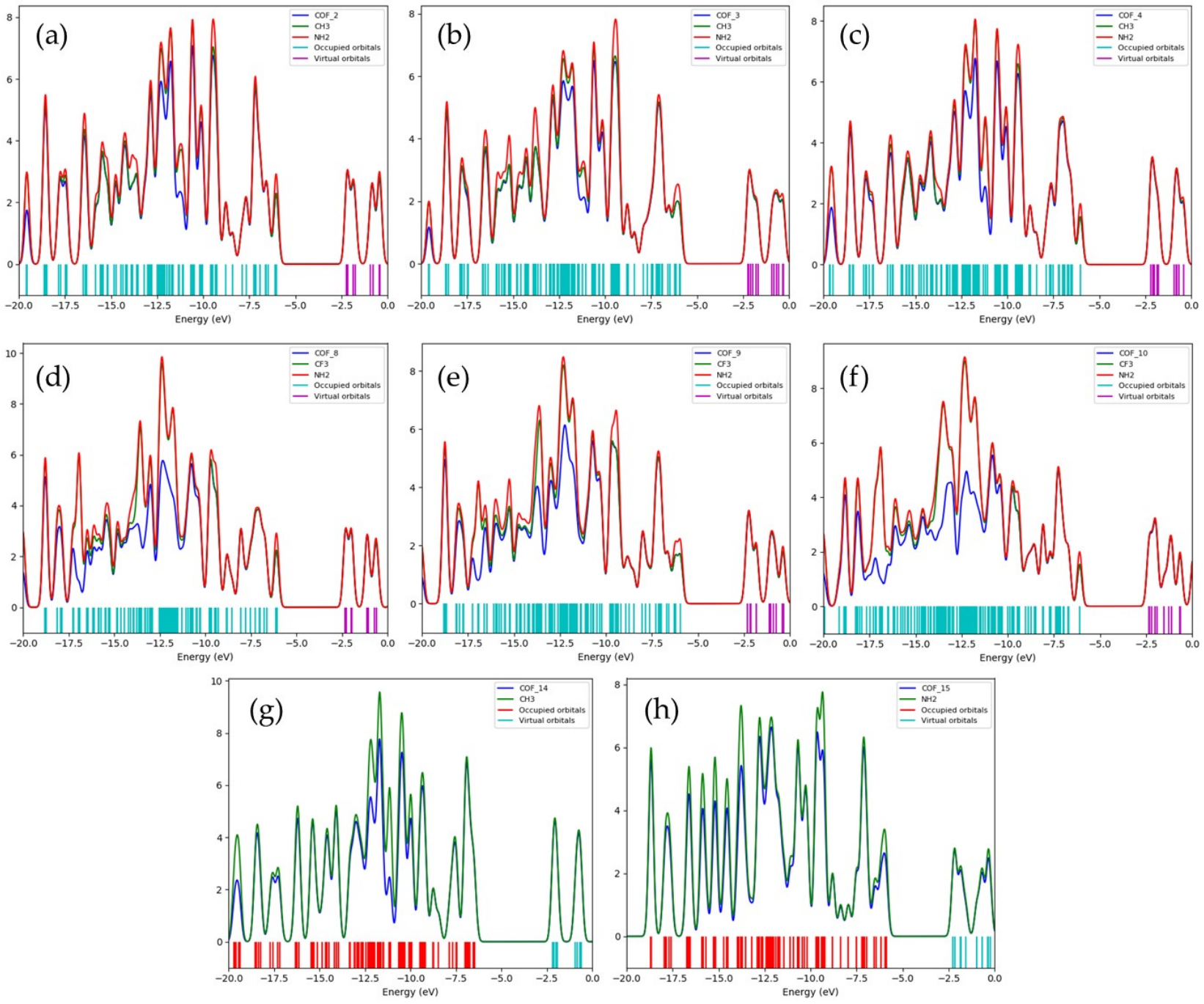


**Figure S5**: Projected Density of States (PDOS) spectra of the investigated (a) MN-COF, (b) $MN_2$-COF, (c) $M_2N$-COF, (d) FN-COF, (e) $FN_2$-COF, (f) $F_2N$-COF, (g) M-COF and (h) N-COF calculated at the M06/6-311g(d) level of theory

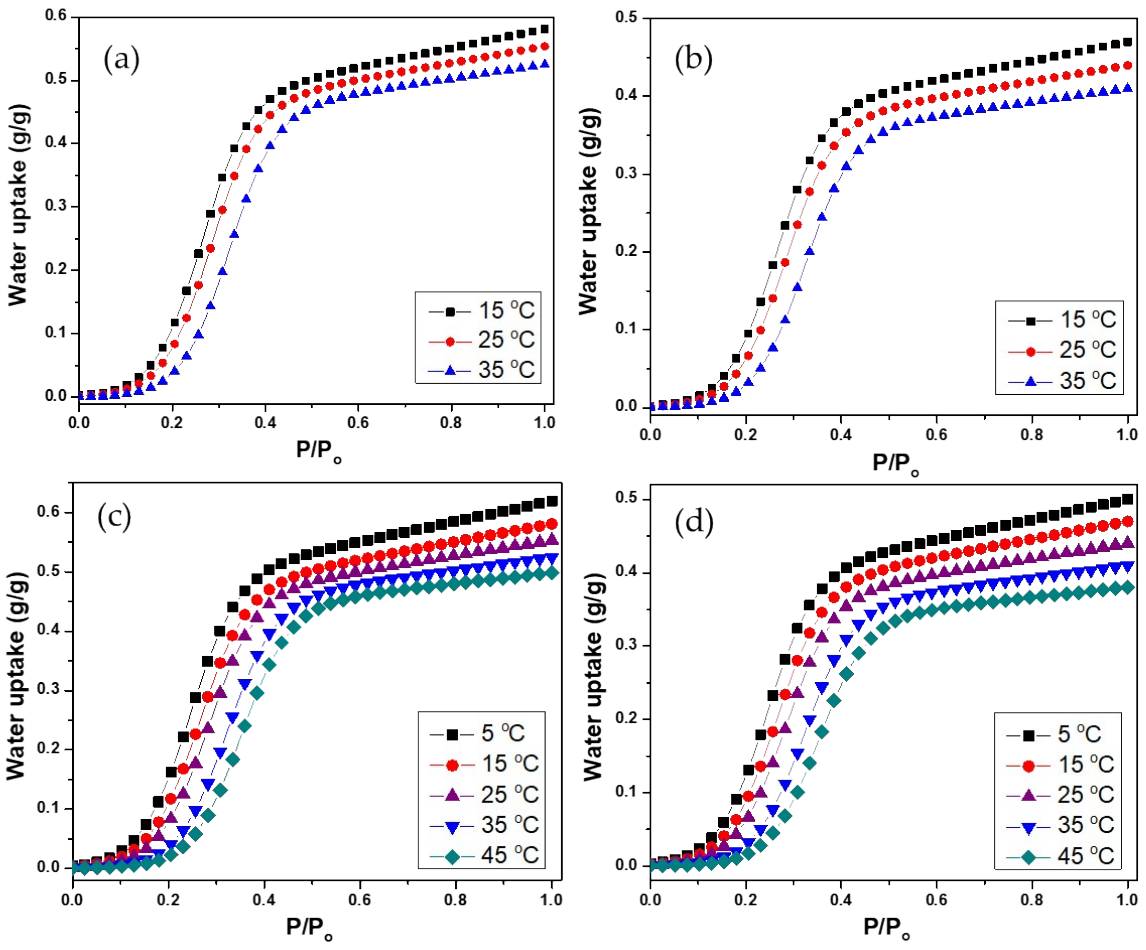


**Figure S6:** Theoretical water adsorption isotherms of AB-COF: (a) raw isotherms at 5-35 °C, (b) scaled isotherms at 5-35 °C after applying the scaling factor, (c) extended unscaled at 5-45 °C, and (d) extended scaled at 5-45 °C.

## Text S1: Determination of Scaling Factors for Theoretical Water Adsorption Isotherms

To enable quantitative comparison between simulated and experimentally measured water adsorption isotherms, a scaling procedure was applied to the theoretical uptake data. This procedure was designed to correct for systematic overestimation of the absolute adsorption capacity observed in the unscaled simulations, while preserving the pressure-dependent shape of the isotherms and their temperature dependence.

For each temperature, a target maximum water uptake was first defined based on the experimentally measured saturation capacity. The target uptake values used in this study were 0.500, 0.470, 0.440, 0.410, and 0.380 g $g^{-1}$ at 5, 15, 25, 35, and 45 °C, respectively. The corresponding maximum uptake values were then extracted from the unscaled theoretical adsorption isotherms obtained at each temperature.

A temperature-dependent scaling factor, $S$, was calculated as the ratio of the experimental saturation uptake to the maximum uptake predicted by the unscaled theoretical isotherm at the same temperature, according to:

$$S = \frac{\text{Target Maximum Uptake}}{\text{Maximum Theoretical Uptake}}$$

The scaling factor was subsequently applied uniformly to the entire theoretical adsorption isotherm at that temperature, such that the scaled uptake was obtained as:

$$q_{\text{scaled}}(P/P_0) = S \times q_{\text{theoretical}}(P/P_0)$$

This approach ensures that the relative pressure dependence and the location of the adsorption step remain unchanged, while the overall magnitude of the uptake is adjusted to match the experimentally observed saturation capacity.

The resulting scaling factors were 0.807494, 0.824702, 0.810440, 0.827246, and 0.762288 at 5, 15, 25, 35, and 45 °C, respectively. These scaling factors were applied consistently to all subsequent theoretical water adsorption isotherms reported in this work.

**Text S2: Reproducibility of the Multiscale Simulation Workflow**

DFT calculations were performed on cluster models extracted from periodic COF structures, with terminal atoms saturated to preserve local chemical environments. The same model construction protocol was applied to all COFs.

GCMC simulations were initialized from empty frameworks for adsorption and from equilibrated high-loading states for desorption. Identical relative humidity sampling schemes were used across all systems.

MD simulations were initialized from equilibrated GCMC snapshots at representative RH conditions and further equilibrated prior to analysis.

This workflow ensures consistent transfer of structural and interaction information across DFT, GCMC, and MD stages and supports reproducibility of the multiscale simulation framework.

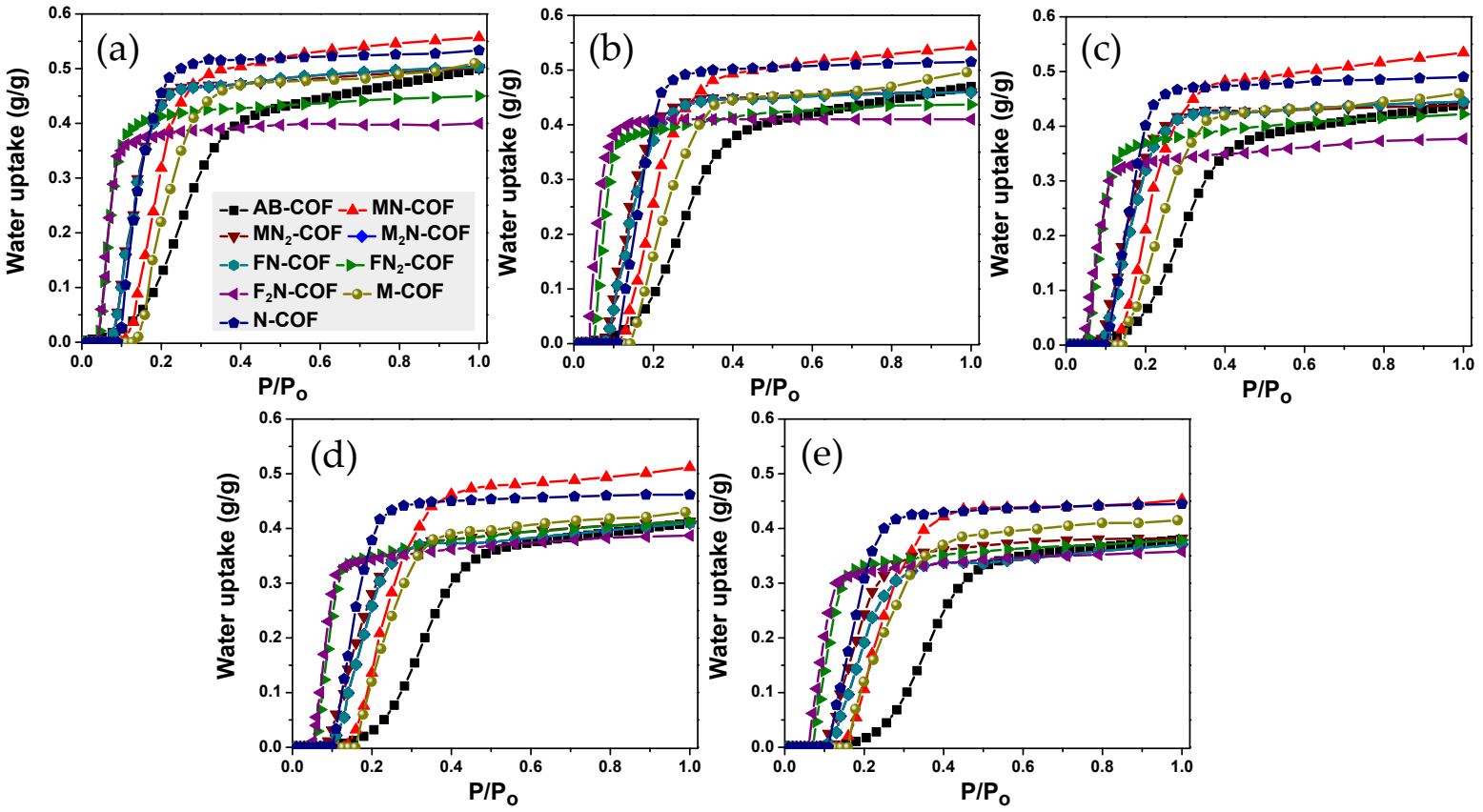


**Figure S7**: Water adsorption isotherms of the investigated COFs at 100% relative humidity and temperatures of (a) 5 $^{o}$C, (b) 15 $^{o}$C, and (c) 25 $^{o}$C, (d) 35 $^{o}$C and (e) 45 $^{o}$C.

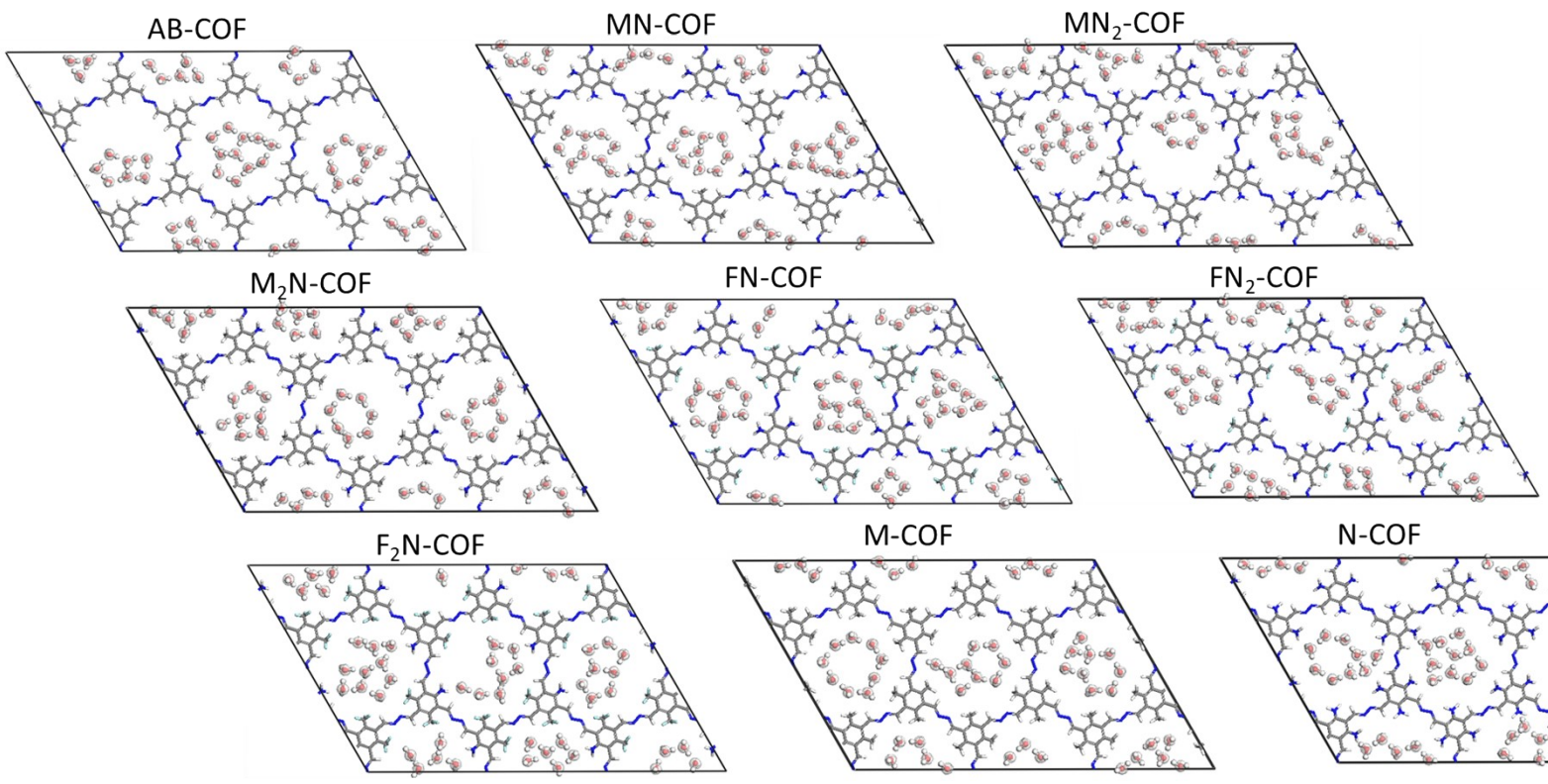


**Figure S8**: Snapshots of water adsorption configurations within the investigated COFs, showing the distribution of water molecules inside the pores.

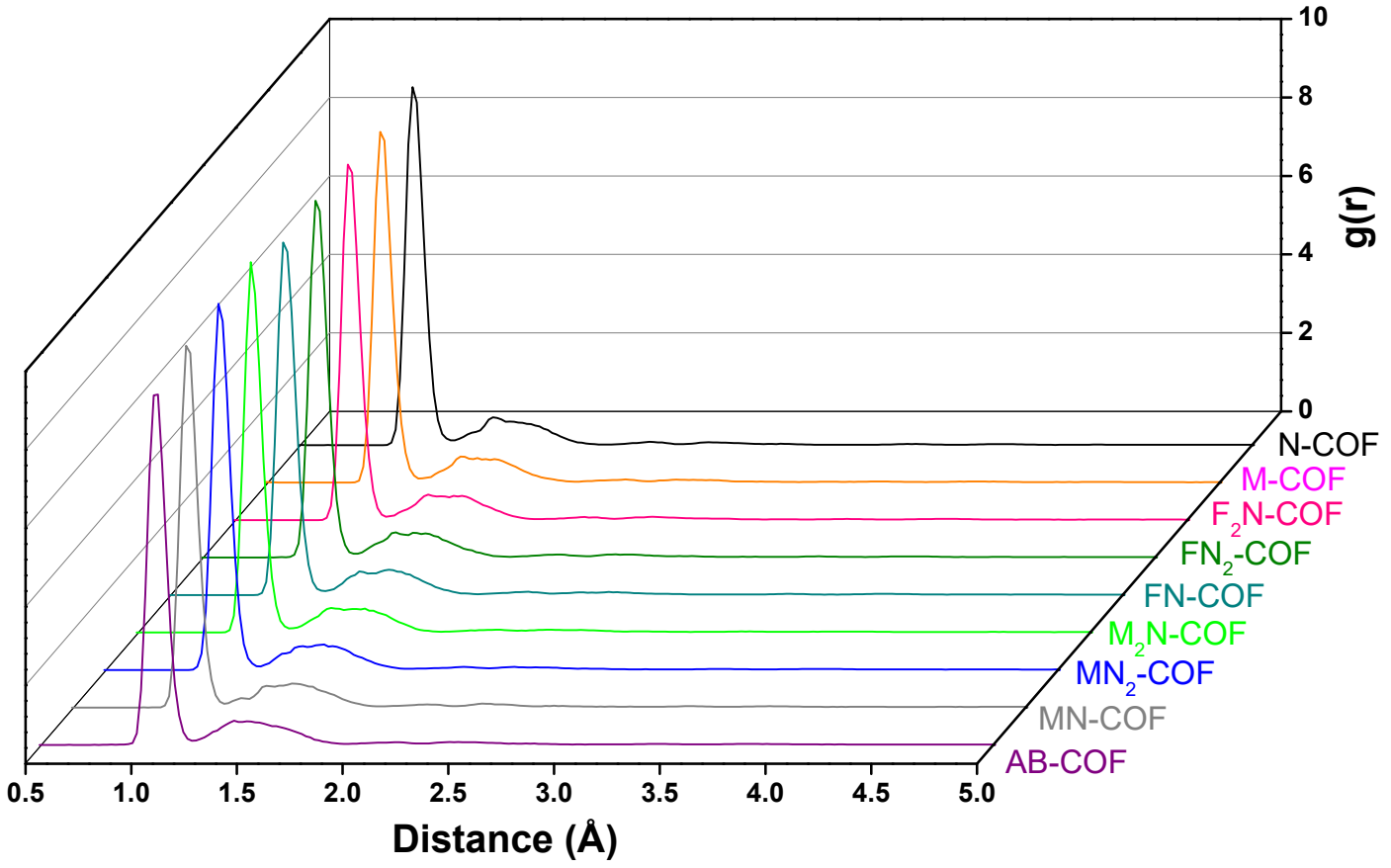


**Figure S9**: Radial distribution functions (RDFs) of water molecules within the investigated COFs, showing the distribution of water–framework interaction distances.

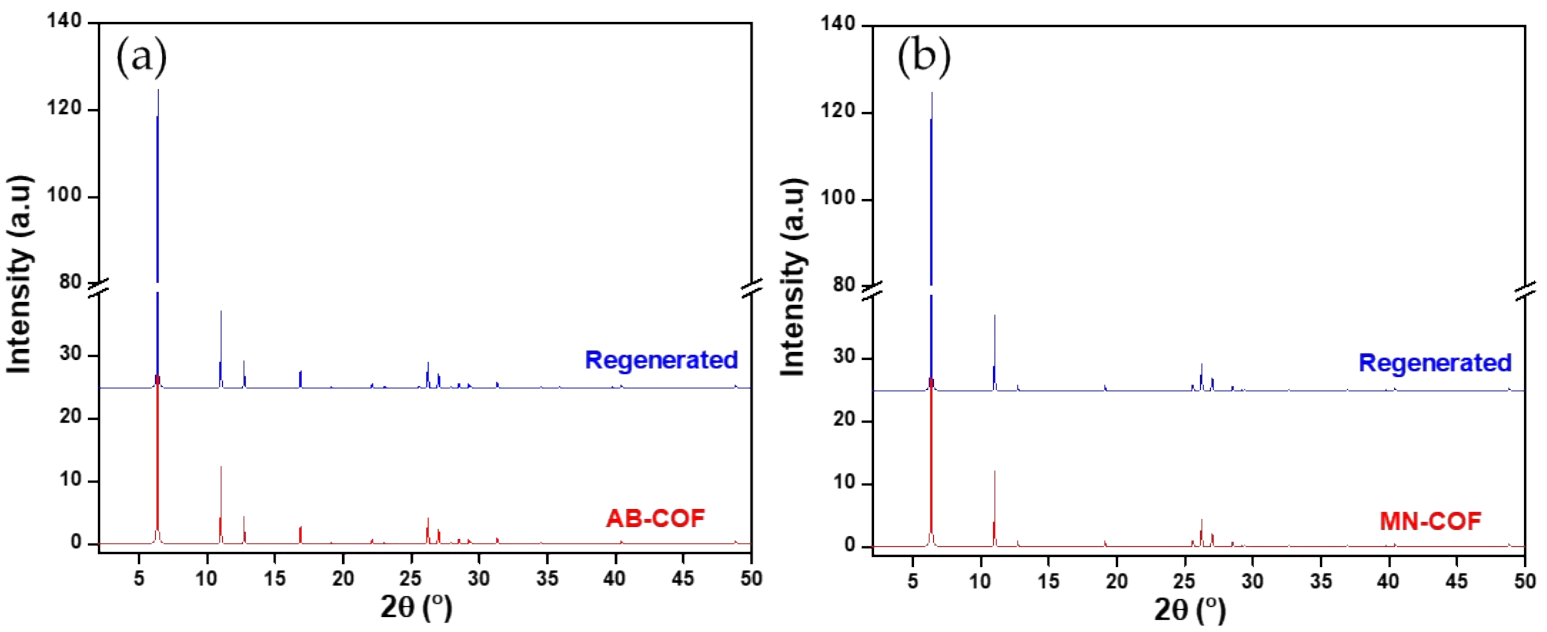


**Figure S10**: PXRD patterns of (a) AB-COF and (b) MN-COF before and after regeneration